CrossMark

ORIGINAL PAPER

# An effective removal of organic dyes using surface functionalized cellulose acetate/graphene oxide composite nanofibers

**Nada M. Aboamera · Alaa Mohamed � · Ahmed Salama · T. A. Osman · A. Khattab**

**Abstract** An effective photocatalyst obtained from composite nanofibers CA/GO fabricated by electrospinning technique followed by chemical crosslinking surface modified $TiO_2$ nanoparticles (NPs) was used for removing the organic dyes Indigo carmine (IC) and Methylene blue (MB) from an aqueous solution under UV irradiation light. The crystalline structure and morphologies of $CA–GO/TiO_2–NH_2$ composite nanofibers were characterized by SEM, TEM, XRD, and FTIR. The prepared $CA–GO/TiO_2–NH_2$ composite nanofibers displayed significantly enhanced photocatalytic activity for photodegradation the organic dyes IC and MB under UV irradiation after 150 and 250 min respectively. The pH value of the solution was studied from 2 to 8 and obtained results showed a clear improvement of photocatalytic activity at pH 2. The results indicated that the activated $CA–GO/TiO_2–NH_2$ composite nanofibers functioned as an adsorbent for the removal of IC and MB from aqueous solutions. In addition, the results showed a high adsorption capacity remain up to 65% after five consecutive capacity cycles.

**Keywords** Graphene oxide · Cellulose acetate · Composite nanofibers · Photocatalytic · Organic contaminants · Electrospinning

N. M. Aboamera · A. Mohamed (✉)
Production Engineering and Printing Technology Department, Akhbar El Yom Academy, Giza 12655, Egypt
e-mail: alakha@kth.se

A. Mohamed
Egypt Nanotechnology Center, EGNC, Cairo University, Giza 12613, Egypt

A. Mohamed
Membrane Technology Department, Institute of Functional Interfaces (IFG), Karlsruhe Institute of Technology (KIT), 76344 Eggenstein-Leopoldshafen, Germany

A. Salama
Department of Production Engineering and Manufacturing Technology, Modern Academy for Engineering and Technology in Maadi, Cairo, Egypt

T. A. Osman · A. Khattab
Mechanical Design and Production Engineering Department, Cairo University, Giza 12613, Egypt

## Introduction

Colored wastewater is a very serious environmental problem. Pigment and organic dye water pollutants are mainly in effluents from industries such as leather, pharmaceutical, textile, rubber, cosmetics, and food industries (Haque et al. 2003; Pan et al. 2010; Mohamed et al. 2016a, b, 2017b, c; Salama et al. 2017). The high toxicity wastewater organic dyes such as indigo carmine and methylene blue which contain aromatic rings cause human health hazards and several environmental pollutions (Gopiraman et al. 2013;

Khalil et al. 2016; Liu et al. 2016; Makama et al. 2016). There are numerous treatment processes, including adsorption, precipitation, electrolysis, chemical coagulation, oxidation liquid membrane separation, and biological treatments that vary in their effectiveness, environmental impacts and costs. These usual treatment techniques were ineffective for removal of such dyes pollution due to its synthetic nature (Azizi et al. 2013; Umar and Aziz 2013; Swaminathan et al. 2014).

Recently, the photocatalytic degradation technique attracted wide attention for removal organic dyes and toxic organic compounds from wastewater than other methods due to its effectiveness, easy operation, lower cost, non-selective degradation and high efficiency (Wu et al. 2012). Photocatalysis is based on absorbing the light of semiconductor oxide photocatalysts such as ZnO and $TiO_2$ by exciting the electrons from the valence band to conduction band then create electron–hole pairs (Karim et al. 2018). Those electrons and holes degrade the organic dye molecules absorbed on the surface of the photocatalyst by starting a redox reaction with water and oxygen (Mohamed et al. 2017a).

$TiO_2$ nanostructure is the most commonly used due its acceptable photocatalytic activity and thermal stability, non-toxicity and relatively low cost (Liu et al. 2017). It was usual using $TiO_2$ as a powder but it was difficult to separate it from the purified water after treatment (Liu et al. 2014; Thunberg 2015). So that, CA/GO composite nanofiber was fabricated by electrospinning method followed by chemical crosslinking of surface modified $TiO_2$ NPs with a high efficiency and high active surface area (Compd 2011). Electrospinning is an effective method due to its potential applications in environmental remediation, photocatalysis, gas sensors, dye sensitized solar cells, and batteries which used to fabricate composite nanofibers with diameters ranging from tens of nanometers to micrometers (Geçgel et al. 2013; Dula et al. 2014). Utilizing CA polymer is usually common due to its relatively easy manufacture, non-toxicity, renewable resource of raw material, and cost effectiveness (Liu and Bai 2006; Kabiri and Namazi 2014; Peng et al. 2014).

The inclusion of graphene oxide (GO) could be a promising strategy for improving the mechanical properties of the nanofibers. Mechanical performance has a great importance for the applications of nanofiber membranes (Yousef et al. 2018). For

instance, sufficient mechanical strength is required to withstand operating and handling conditions. The most important graphene derivative is GO. GO has a large number of hydrophilic groups on its surface, such as carboxyl, hydroxyl and epoxy if compared with graphene (Yuan et al. 2013). GO is highly negatively charged in water due to the deprotonation of these oxygen-containing groups. GO was used due to its graphitic structure, unique mechanical property, electrical conductivity and thermal conductivity (Uhl and Wilkie 2002; Lee et al. 2008). Furthermore, GO provide the potential of cost effective and large scale production of graphene based materials (Zhu et al. 2010).

In this paper, CA/GO composite nanofibers were fabricated by using electrospinning techniques. In order to enhance the degradation efficiency of dye pollutants, the surface of CA/GO composite nanofibers was chemically crosslinked by the photocatalytic $TiO_2$ NPs. The fabricated CA/GO composite nanofibers crosslinked by $TiO_2$ was tested for the photodegradation of two organic dyes IC and MB under ultraviolet light irradiation. The degradation of IC and MB were studied by investigating the degradation influencing factors such as irradiation time, pH of the solution, initial dyes concentration, and the photocatalyst amount. All these factors were studied in order to get the optimum photodegradation conditions.

## Experimental

### Materials

Graphene oxide (GO) was purchased from XF Nano, Inc. Cellulose acetate (CA, 39.7% acetyl content, average $M_w$ = 50,000) was obtained from Sigma Aldrich Chemical Company. Titanium dioxide powder ($TiO_2$ Degussa P-25). Acetone, Dimethylformamide (DMF), 3-Aminpropyltriethoxysilane (APTES), Methanol, Glutaraldehyde (GA), Toluene, Indigo carmine (IC) and methylene blue (MB) were purchased from sigma Aldrich and used directly without further purification.

### Preparation of composite nanofibers

According to our previous work, GO was incorporated into CA with different weight percentages of GO

(0.05, 0.5, 1 and 1.5 wt%) by using the electrospinning technique. GO with 1.5 wt% was chosen for our experimental work due to its high capacity to improve the mechanical properties for composite nanofibers (Aboamera et al. 2017). Firstly, we prepared the electrospinning solution which was composed of 15 wt% cellulose acetate (CA), 1.5 wt% graphene oxide (GO) and then dissolved in a solvent mixture of dimethylformamide (DMF) and acetone (2:3 by weight). In order to get a homogenous solution and improve the mixture solubility, the electrospinning solution was applied under sonication for 4 h at 60 °C and then subjected overnight under magnetic stirring at 40 °C. To form the CA/GO composite nanofibers, the electrospinning solution was placed into a syringe pump with 0.5 mm inner diameter of the capillary tip and the stainless steel spinneret was connected to the positive electrode. An electric field generated from a high voltage–power supply (0–30 kV). A stainless steel plate attached to an aluminum foil was used as the collector and was connected to the ground. The applied flow rate was 0.13 mL/h, the voltage was adjusted at 27 kV, the distance between tip and collector was 15 cm and the experiment was conducted at room temperature. The obtained fiber was dried at 80 °C under vacuum for 12 h to remove all the solvent residues.

In order to improve the efficiency of TiO$_2$ photocatalyst, the surface of TiO$_2$ NPs was modified with the amino group NH$_2$ by adding 0.5 g of TiO$_2$ NPs to 100 mL of toluene and then applied the mixture for sonication for 30 min. Then, 3 mL of silane coupling agent was added to the TiO$_2$ suspension and refluxed at 110 °C for 24 h that produced a functional group NH$_2$ on the TiO$_2$ NPs surface. Finally, the surface modified TiO$_2$ NPs was washed with deionized water and methanol then centrifuged until dry (Xiang et al. 2013; Dadvar et al. 2017). In addition, to carry out a chemical crosslinking for the CA/GO composite nanofibers these fibers immersed into 2.5 wt% Glutaraldehyde (GA), then applied to a shaker system for 24 h at room temperature followed by washing and drying. After that, 2 mL of an aqueous dispersion of TiO$_2$–NH$_2$ NPs was added and then applied to a shaker system for 24 h. Finally, the chemical crosslinking composite nanofibers were washed and dried. Figure 1 illustrated the complete preparation process of CA–GO/TiO$_2$–NH$_2$ composite nanofibers.

## Characterizations

The surface morphologies and microstructure of CA and CA–GO/TiO$_2$–NH$_2$ composite nanofibers were measured by scanning electron microscope (SEM; Quanta FEG 250, Republic Czech) and Transmission Electron Microscopy (TEM, JEM-2100F, Joel). The crystalline structures were examined by X-ray diffraction (XRD, Bruker D8 advance X-ray diffractometer). Fourier Transform Infrared Spectroscopy (FTIR, JASCO, ft-ir6100, Japan) was used to confirm the attachment between TiO$_2$-NH$_2$ NPs and CA/GO composite nanofibers and studied its affection on the crystalline phases. Thermogravimetric analysis (TGA) curves were measured by using an SDT Q600 thermogravimetric analyzer from room temperature to 800 °C with a heating rate of 20 °C/min and an air flow rate of 100 mL/min.

## Photodegradation experiment

Organic dyes IC and MB were used to evaluate the photocatalytic degradation performance of CA–GO/TiO$_2$–NH$_2$ composite nanofibers under UV light irradiation by using a UV-lamp (40 W, with a wavelength range from 320 to 400 nm). Photocatalytic composite nanofibers containing 1:3 weight ratio of TiO$_2$ and GO was mixed with the organic dyes that have a mass concentration of 10 mg/L IC, or 10 mg/L MB and then applied for a shaker system for 30 min in the dark for establishing the adsorption–desorption equilibrium at room temperature. The pH value of the organic dye solution was adjusted by using HCl with a value between 2 and 8 to study the pH effect on the photodegradation experiments. After that, the mixture was exposed to the UV light irradiation under ambient conditions. At a fixed time interval, about 3 mL suspensions were withdrawn from the mixture for the UV absorption spectrum analysis on a Varian Cary-50 UV–Vis spectrophotometer. The degradation efficiency of IC and MB was calculated by the following Eq. (1).

$$\text{Degradation efficiency}(\%) = \frac{C_i - C_0}{C_i} * 100 \qquad (1)$$

where, $C_i$ (mg/L) is the initial concentration of IC and MB before irradiation, and $C_0$ (mg/L) is the concentration of IC and MB solution measured after irradiation.
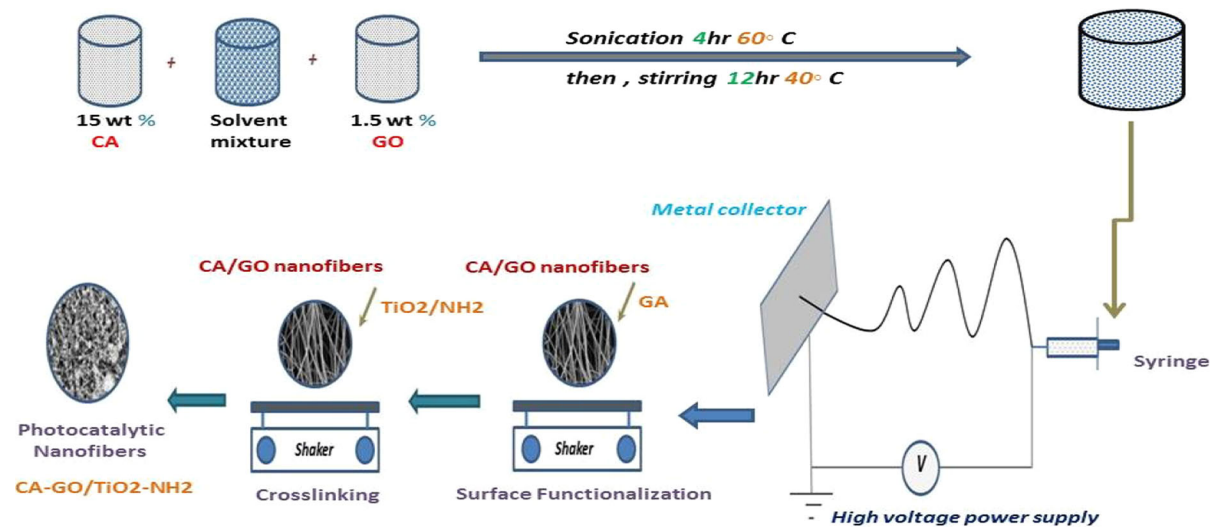
**Fig. 1** Schematic diagram illustrating the preparation of CA–GO/TiO$_2$–NH$_2$ composite nanofibers

## Results and discussion

Characterization and morphologies of nanofibers

A scanning electron microscope (SEM) technique was used to study the morphologies of CA and CA–GO/TiO$_2$–NH$_2$ nanofibers as shown in Fig. 2. It can be seen that the pure CA nanofibers shown in Fig. 2a are fine, uniform and perspicuous with average diameters of about 300 nm. The SEM images for CA–GO/TiO$_2$–NH$_2$ composite nanofibers show a coarse surface and porous structure as a result of the crosslinking attached between the amino functionalized TiO$_2$ NPs and the composite nanofibers CA/GO as shown in Fig. 2b. The overview FE-SEM image of CA–GO/TiO$_2$–NH$_2$ composite nanofibers sample shows a complex network structure and the resulting nanofibers were composed of many randomly intersecting microfibers with high aspect ratios as a result of TiO$_2$–NH$_2$ NPs addition. Also, the surface morphologies of CA/GO–TiO$_2$–NH$_2$ composite nanofibers were examined using Transmission Electron Microscopy (TEM). Figure 3 shows TEM images with different magnification which, illustrate the aggregation of small TiO$_2$ NPs along the fibers and show a homogeneous dispersion of TiO$_2$–NH$_2$ NPs into the composite nanofibers CA/GO.

In addition, X-ray diffraction (XRD) was used to identify the crystalline phases present in the CA–GO/TiO$_2$–NH$_2$ nanofibers as shown in Fig. 4. The results

showed that the reflection peak of CA was found at 16.55°. In addition, the peaks at 36.23°, 47.43°, 56.61°, 62.77°, and 67.95° confirmed the presence of TiO$_2$. Furthermore, FTIR spectra were applied to investigate materials interactions and the characterization of absorbance data for CA and CA–GO/TiO$_2$–NH$_2$ nanofibers as shown in Fig. 5. FTIR spectra of pure CA nanofibers exhibited two absorption bands of OH and C–H group stretching at 3503 and 2946 cm$^{-1}$ respectively and also showed characteristics peaks at 1761, 905 and 604 cm$^{-1}$ due to the stretching of C=O, C–CH$_3$ and C–O–C, respectively as shown in Fig. 5a. It is clear that the peaks of CA spectra are shifted to 3498, 2949, 1753, 908, 605 cm$^{-1}$ spectra of CA–GO/TiO$_2$–NH$_2$ composite nanofibers Fig. 5b. This shift in the absorption bands confirmed the formation of composite material. The peaks observed at 1249, 1078 cm$^{-1}$ are assigned to NH$_2$ group and N–H stretching respectively (VanderHart et al. 1996).

Moreover, the TGA/DTG analyses of CA–GO/TiO$_2$–NH$_2$ composite nanofibers were shown in Fig. 6. It can be seen that the weight loss from 290 to 720 °C, could be attributed to the combustion and decomposition of composite nanofibers occurred in this temperature range.

Photocatalytic activity

The catalyst material is an important parameter which affects the photodegradation performance. In this
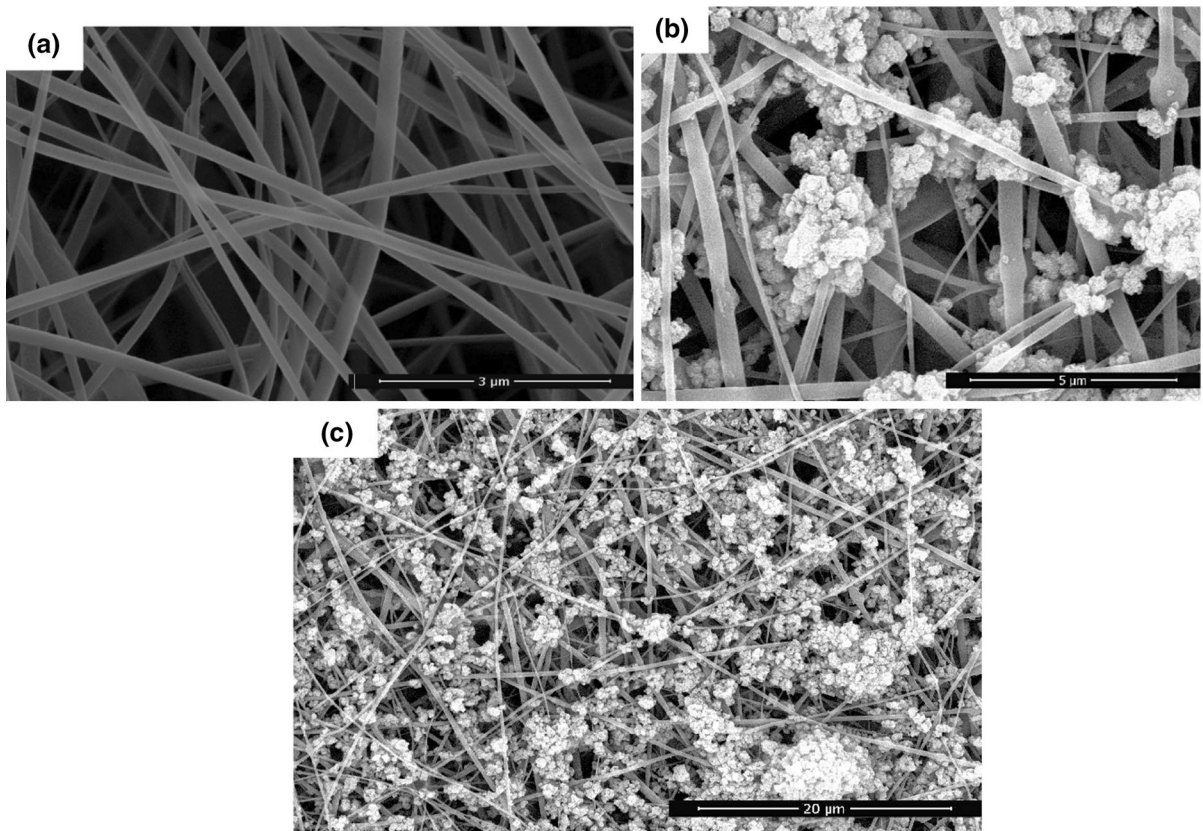
Fig. 2 SEM images of the fabricated nanofibers **a** CA, **b** CA–GO/TiO$_2$–NH$_2$ and **c** FE-SEM for CA–GO/TiO$_2$–NH$_2$
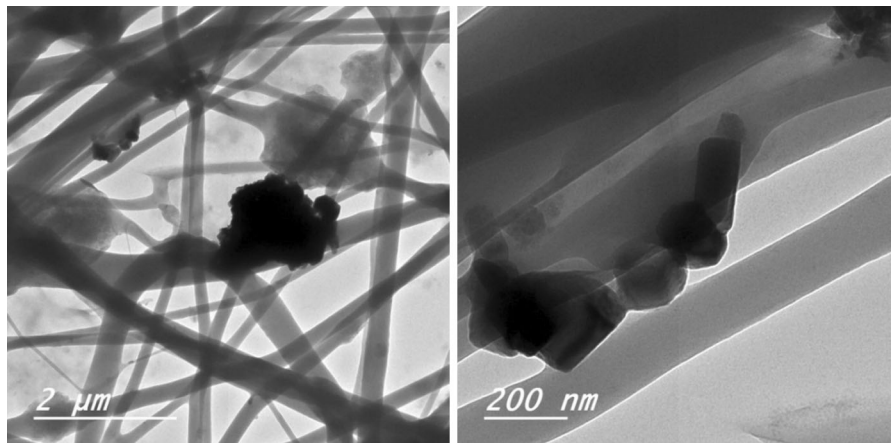


Fig. 3 TEM images of CA/GO–TiO$_2$–NH$_2$ composite nanofibers with different magnification

regards, TiO$_2$ photocatalyst is the most promising material because of its wide band gap and high photosensitivity (Liu et al. 2016). Irradiation time and source of power intensity should be considered for designing highly efficient photocatalyst. Here, we

evaluate the photocatalytic performance of the as-prepared CA–GO/TiO$_2$–NH$_2$ composite nanofibers by monitoring the degradation of 10 mg/L IC and 10 mg/L MB from the aqueous solutions at pH 2 under (40 W) UV source of light intensity at room
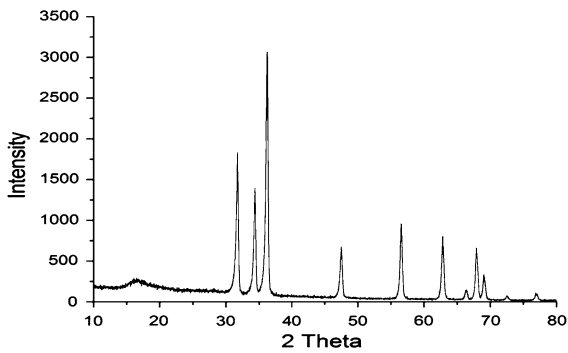
**Fig. 4** XRD diffraction patterns of CA–GO/TiO$_2$–NH$_2$ nanofibers

temperature. Before irradiation, the solution of organic dyes and the catalyst were put in a shaker in a dark for 30 min to ensure that the dyes IC and MB were absorbed to a saturation on the surface of the catalyst (Karthikeyan et al. 2005). Figure 7 shows the gradually fades of the color of the solution with the increasing of time, which implies the gradual decrease of IC and MB concentration in the mixture. In addition, the photodegradation performance of IC and MB was determined from the results obtained from UV–vis spectroscopy. The results obtained are shown in Fig. 8 in which the peak at 610 and 664 nm corresponding to IC and MB. Moreover, Fig. 9 shows



**Fig. 5** FTIR spectra of **a** CA nanofibers and **b** CA–GO/TiO$_2$–NH$_2$ composite nanofibers
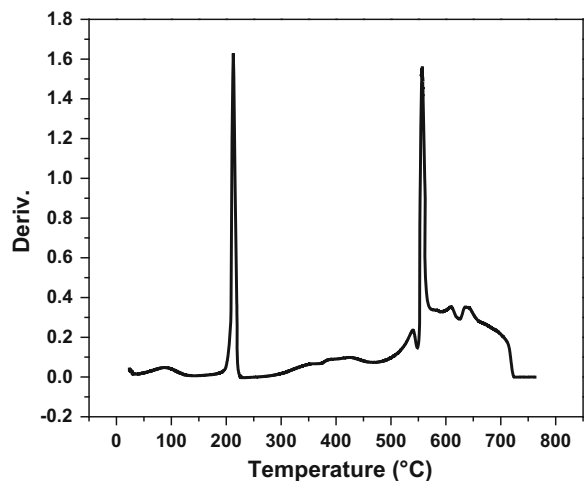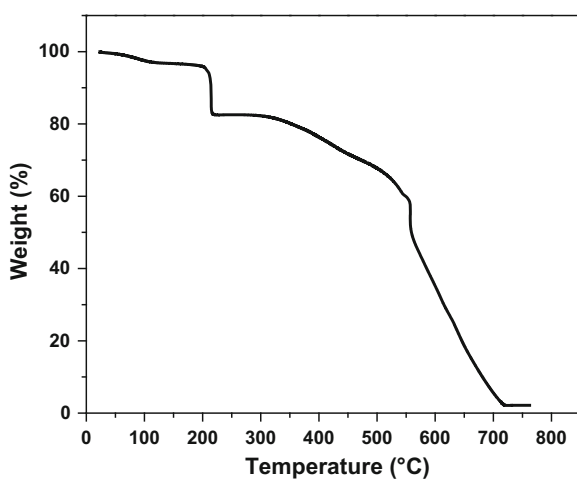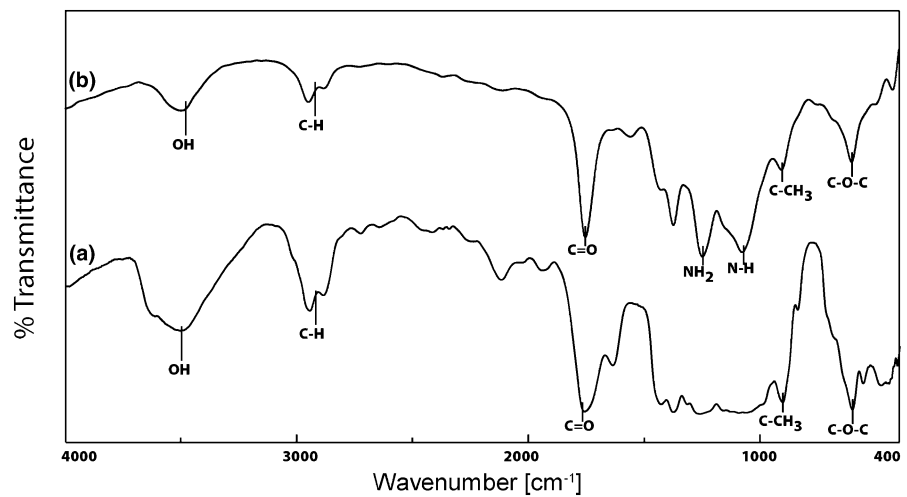


**Fig. 6** TGA analysis of CA–GO/TiO$_2$–NH$_2$ composite nanofibers

**Fig. 7** The solutions color changing with the time increasing
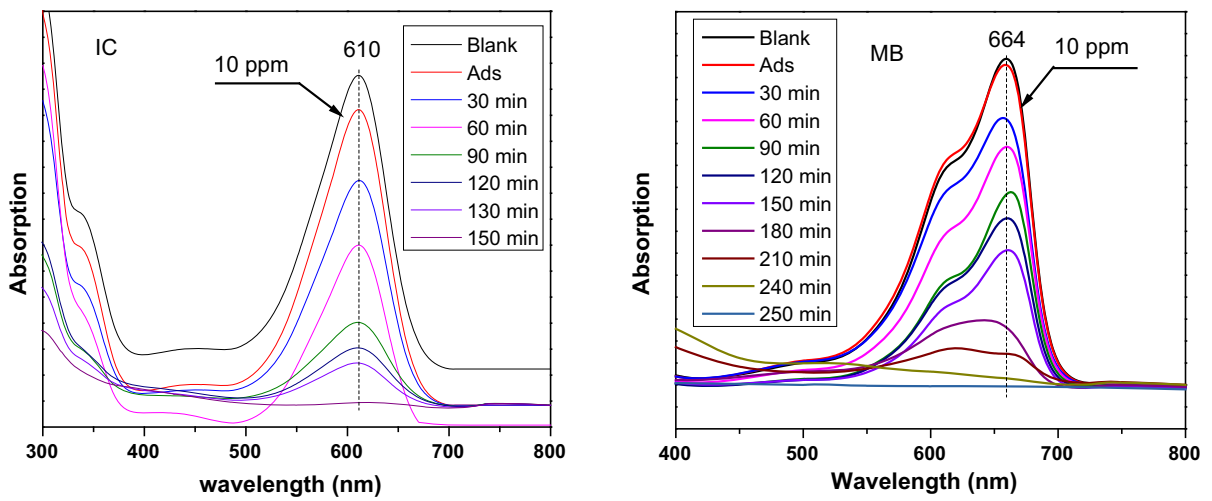


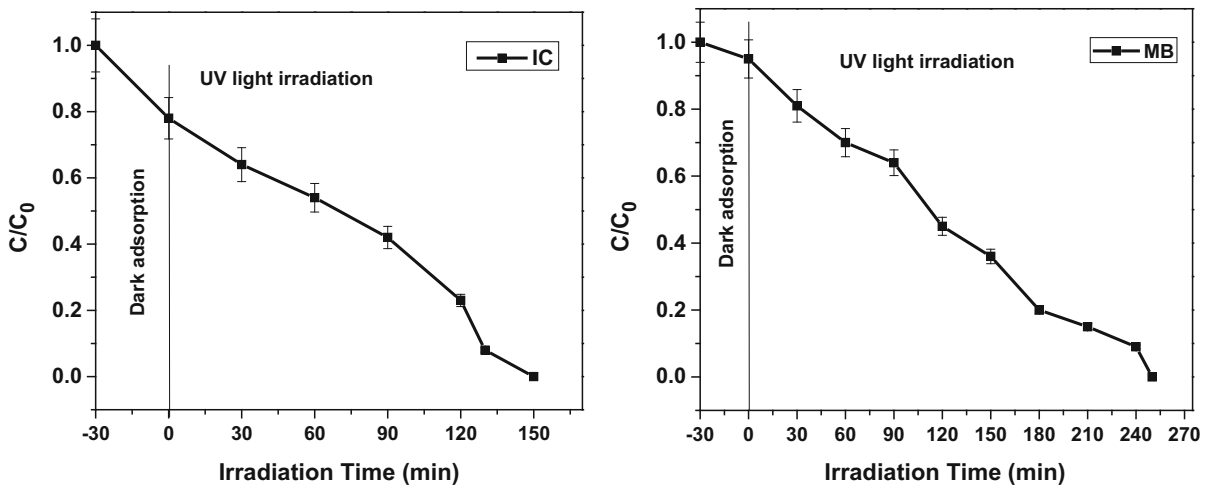**Fig. 8** UV–vis curves of IC and MB under UV light irradiation



**Fig. 9** Photodegradation efficiency of CA–GO/TiO$_2$–NH$_2$ composite nanofibers as a function of irradiation time for removing IC and MB

the photodegradation efficiency of CA–GO/TiO$_2$–NH$_2$ composite nanofibers as a function of irradiation time for removing the IC and MB. The photodegradation values were represented by C/C$_0$, where C$_0$ is the initial concentration of IC and MB solutions before UV irradiation, and C is the concentration of IC and MB solutions measured at fixed time after UV irradiation. The results showed that the CA–GO/TiO$_2$–NH$_2$ composite nanofibers degraded about 36% after 30 min for IC, while for MB degraded about 20% under the same experimental condition. Degradation of the organic dyes IC and MB under UV light irradiation are almost complete after 150 and 250 min respectively at the lowest dye concentration (10 ppm), under UV light irradiation (40 W) and at a pH value of 2.

Moreover, pseudo-first order kinetics equation was applied to analyse the photodegradation of IC and MB kinetics data using CA–GO/TiO$_2$–NH$_2$ composite nanofibers (Wang et al. 2006). The equation is expressed as the following:

$$\ln\left(\frac{C_0}{C}\right) = k_a t \qquad (2)$$

where, C$_0$ (mg/L) is the initial concentration of the dye solution before irradiation, C (mg/L) is the concentration of the dye solution after irradiation at a time interval t (min), and K$_a$ (min$^{-1}$) is the apparent rate constant. The constant K$_a$ value was resulted from the slope of the plot ln (C$_0$/C) as a function of irradiation

**Table 1** Kinetic parameters obtained for the degradation of IC and MB on CA–GO/TiO$_2$–NH$_2$ composite nanofibers

| Photocatalyst | $K_a$ (min$^{-1}$) | | $R^2$ | |
|---|---|---|---|---|
| | IC | MB | IC | MB |
| CA–GO/TiO$_2$–NH$_2$ | 0.009 | 0.006 | 0.959 | 0.964 |

time Fig. 10. Pseudo-first order rate constant for the photocatalytic degradation of the organic dyes IC and MB was listed in Table 1. In addition, the Ka value of IC was found higher than MB because of the different chemical structure of each dye and also due to the anionic type of IC and the cationic type of MB (Lu et al. 1993). The resulted kinetic data can be represented as a large active binding sites on the TiO$_2$ NPs catalyst surface and the photocatalyst exposure to the dye solution and UV light irradiation (Al-Degs et al. 2001).

Furthermore, the pH value of the solution was discussed due to its effect on the surface state of the adsorbent and also on the exciting forms of the adsorbate. The effect of change of the pH value from 2 to 8 on the photodegradation of IC and MB by using CA–GO/TiO$_2$–NH$_2$ nanofibers are plotted in Fig. 11. The degradation of IC and MB showed high degradation efficiency in a short irradiation time at pH 2. The maximum removal of IC was 99.8 and 72% in the pH range from 2 to 8, while 98.3 and 51% for MB in the same pH range. This effect of changes pH values due to the electrostatic interaction between positively
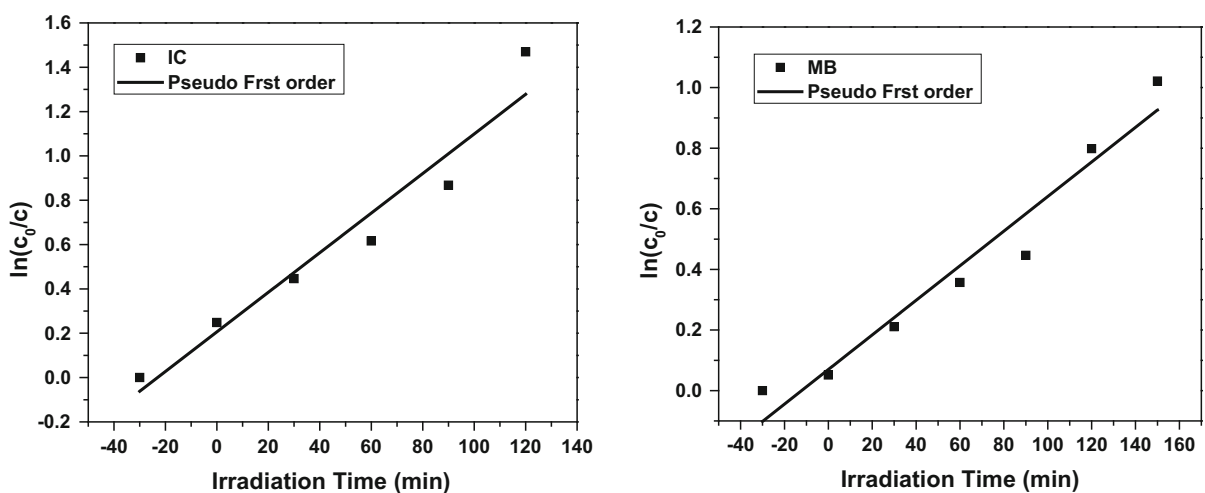


**Fig. 10** Photodegradation kinetics of CA–GO/TiO$_2$–NH$_2$ composite nanofibers as a function of irradiation time for removing IC and MB
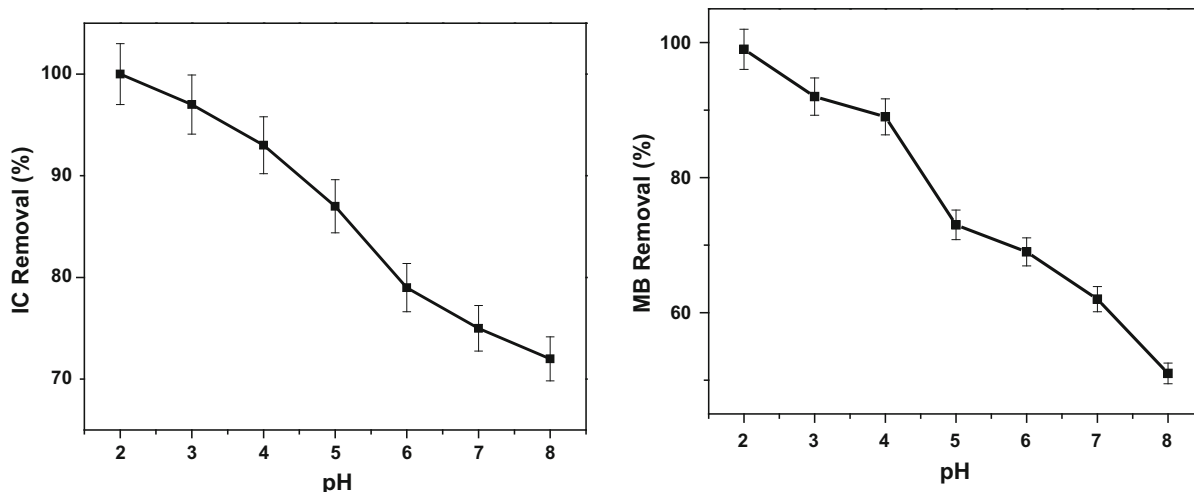
**Fig. 11** Effect of pH on IC and MB using CA–GO/TiO$_2$–NH$_2$ composite nanofibers

**Table 2** Comparison of maximum IC and MB adsorption

| Adsorbent | Dyes Concentration mg/l | | Irradiation light | Equilibrium time (min) | | References |
|---|---|---|---|---|---|---|
| | IC | MB | | IC | MB | |
| PAN/CNTs | 10 | 10 | UV 100 W | 60 | 120 | Mohamed et al. (2017c) |
| PAN–CNT/TiO$_2$–NH$_2$ | 10 | 10 | UV 100 W | 10 | 30 | Mohamed et al. (2016a) |
| PAN/1.5 wt% GO | – | 10 | UV 125 W | – | 420 | Swaminathan et al. (2014) |
| carbon-doped TiO$_2$ coating on MWCNTs | – | 20 | Visible light 500 W | – | 360 | Cong et al. (2011) |
| TiO$_2$ nanofibers | – | 10 | UV 120 W | – | 600 | Bubacz et al. (2010) |
| CNT-embedded hollow TiO$_2$ | – | 10 | UV 800 W | – | 70 | Jung et al. (2015) |
| CA–CNT/TiO$_2$–NH$_2$ | 10 | 10 | UV 40 W | 180 | 300 | Salama et al. (2018) |
| CA–GO/TiO$_2$–NH$_2$ | 10 | 10 | UV 40 W | 150 | 250 | This work |

charged amine groups and negatively charged of IC and MB species. Table 2 lists the maximum adsorption capacities of IC and MB for CA–GO/TiO$_2$–NH$_2$ composite nanofibers and other related adsorbents reported in the literature. The data indicates that the prepared CA–GO/TiO$_2$–NH$_2$ composite nanofibers show higher adsorption capacity of IC and MB than many other reported adsorbents. The experimental results for CA–GO/TiO$_2$–NH$_2$ composite nanofibers showed high effective degradation for organic dyes and stable adsorption capacity can remain up for numerous consecutive cycles (Miller et al. 2011).

The activity of the photocatalysis processes depends on the amount of the adsorption dyes on the catalyst surface. The organic dyes adsorption depends
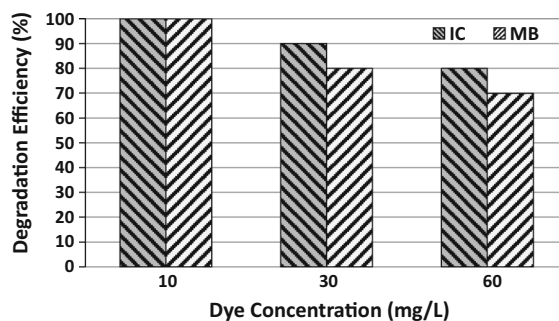


**Fig. 12** The effect of organic dyes initial concentration on the photodegradation efficiency for IC and MB
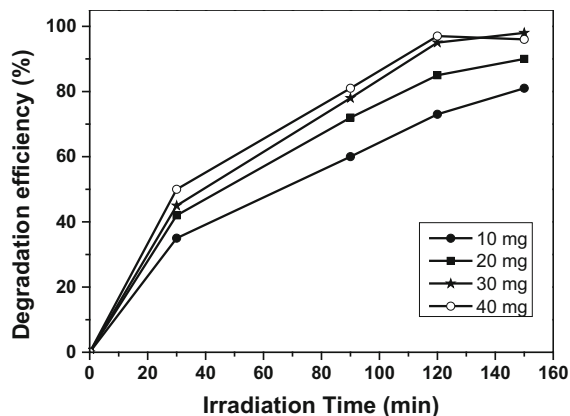
**Fig. 13** Effect of catalyst dose on the degradation efficiency of IC, under UV light irradiation

on the initial concentration of dyes. The initial concentration of dyes at photocatalysis process is an important factor which has to be taken into account. Figure 12 shows the effect of initial concentration organic dyes on the photodegradation efficiency for IC and MB. At the increase of the initial dyes concentration from 10 to 60 ppm the degradation efficiencies were decreased about 20% for IC and about 30% at MB. The decrease in degradation percentage resulted because of as the initial dyes concentration increase the amount of organic substances are adsorbed on the catalyst surface and reduce the photons number to reach the catalyst surface, also reduced the formation of hydroxyl radicals (Zaleska 2008). As a result, the photodegradation percentage was decreased with the increase of dye concentration, while the amount of catalyst was kept constant.

The amount of catalyst is one of the important reaction parameters which affect the reaction efficiency by increasing conversion. To study the catalyst effect on the IC removal performance, different amount of CA–GO/TiO$_2$–NH$_2$ mats was added into 10 ppm IC solution at pH 2. The results indicated that the percentage removal of IC rapidly increased with the increase of mat dosage from 10 to 40 mg as shown in Fig. 13. The increase of percentage removal of IC was due to the more available sorption sites. However, when the dosage of CA–GO/TiO$_2$–NH$_2$ mats was more than 30 mg, the percentage removal of IC was slightly increased.

## Conclusions

At the end of our work, the prepared CA–GO/TiO$_2$–NH$_2$ composite nanofibers improved the degradation performance of the contamination dyes IC and MB from an aqueous solution. The photodegradation experiment was enhanced due to the chemical crosslinking interaction between the electrospinning CA/GO and the amino functionalized TiO$_2$–NPs. In our work, we demonstrate the superior degradation efficiency under UV light irradiation for removing IC and MB at pH 2. The maximum degradation efficiency was achieved after 150 and 250 min for IC and MB respectively. The prepared CA–GO/TiO$_2$–NH$_2$ composite nanofibers show a stable adsorption capacity for many degradation cycles, fast adsorption rate, and using low power intensity.

## References

Aboamera NM, Mohamed A, Salama A et al (2017) Characterization and mechanical properties of electrospun cellulose acetate/graphene oxide composite nanofibers. Mech Adv Mater Struct. https://doi.org/10.1080/15376494.2017.1410914

Al-Degs Y, Khraisheh MAM, Allen SJ, Ahmad MNA (2001) Sorption behavior of cationic and anionic dyes from aqueous solution on different types of activated carbons. Sep Sci Technol 36:91–102

Azizi S, Ahmad M, Mahdavi M, Abdolmohammadi S (2013) Preparation, characterization, and antimicrobial activities of ZnO nanoparticles/cellulose nanocrystal nanocomposites. BioResources 8:1841–1851

Bubacz K, Choina J, Dolat D, Morawski AW (2010) Methylene blue and phenol photocatalytic degradation on nanoparticles of anatase TiO$_2$. Pol J Environ Stud 19:685–691. https://doi.org/10.1016/j.matlet.2011.06.005

Compd JA (2011) Enhanced photocatalytic degradation of methylene blue by ZnO-reduced graphene oxide composite synthesized via microwave. J Alloys Compund. https://doi.org/10.1016/j.jallcom.2011.08.045

Cong Y, Li X, Qin Y et al (2011) Carbon-doped TiO$_2$ coating on multiwalled carbon nanotubes with higher visible light photocatalytic activity. Appl Catal B Environ 107:128–134. https://doi.org/10.1016/j.apcatb.2011.07.005

Dadvar E, Kalantary RR, Ahmad Panahi H, Peyravi M (2017) Efficiency of polymeric membrane graphene oxide-TiO$_2$ for removal of azo dye. J Chem 2017:6217987. https://doi.org/10.1155/2017/6217987

Dula T, Siraj K, Kitte SA (2014) Adsorption of hexavalent chromium from aqueous solution using chemically

activated carbon prepared from locally available waste of bamboo (*Oxytenanthera abyssinica*)

Geçgel Ü, Özcan G, Gürpınar GÇ (2013) Removal of methylene blue from aqueous solution by activated carbon prepared from pea shells (*Pisum sativum*). J Chem 2013:614083. https://doi.org/10.1155/2013/614083

Gopiraman M, Fujimori K, Zeeshan K et al (2013) Structural and mechanical properties of cellulose acetate/graphene hybrid nanofibers: spectroscopic investigations. Express Polym Lett 7:554–563. https://doi.org/10.3144/expresspolymlett.2013.52

Haque MM, Bahnemann D, Muneer M (2003) photocatalytic degradation of organic pollutants. Mech Kinet 3

Jung JY, Lee D, Lee YS (2015) CNT-embedded hollow $TiO_2$ nanofibers with high adsorption and photocatalytic activity under UV irradiation. J Alloys Compd 622:651–656. https://doi.org/10.1016/j.jallcom.2014.09.068

Kabiri R, Namazi H (2014) Nanocrystalline cellulose acetate (NCCA)/graphene oxide (GO) nanocomposites with enhanced mechanical properties and barrier against water vapor. Cellulose. https://doi.org/10.1007/s10570-014-0366-4

Karim SA, Mohamed A, Abdel-Mottaleb MM et al (2018) Mechanical properties and the characterization of poly-acrylonitrile/carbon nanotube composite nanofiber. Arab J Sci Eng. https://doi.org/10.1007/s13369-018-3065-x

Karthikeyan T, Rajgopal S, Miranda LR (2005) Chromium (VI) adsorption from aqueous solution by Hevea Brasilinesis sawdust activated carbon. J Hazard Mater 124:192–199

Khalil W, Mohamed A, Bayoumi M, Osman TA (2016) Tribological properties of dispersed carbon nanotubes in lubricant. Fuller Nanotub Carbon Nanostruct. https://doi.org/10.1080/1536383X.2016.1188804

Lee C, Wei X, Kysar JW, Hone J (2008) Measurement of the elastic properties and intrinsic strength of monolayer graphene. Science 321:385–388. https://doi.org/10.1126/science.1157996

Liu C, Bai R (2006) Adsorptive removal of copper ions with highly porous chitosan/cellulose acetate blend hollow fiber membranes. J Memb Sci 284:313–322

Liu G, Liu S, Lu Q et al (2014) BiVO4/cobalt phthalocyanine (CoPc) nanofiber heterostructures: synthesis, characterization and application in photodegradation of methylene blue. RSC Adv 4:53402–53406. https://doi.org/10.1039/C4RA08759C

Liu H, Zhang Y, Yang H et al (2016) Study on synthesis and photocatalytic activity of porous titania nanotubes. Adv Mater Sci Eng. https://doi.org/10.1155/2016/3532817

Liu M, Liu Y, Zhang D et al (2017) Facile fabrication of H2BDC-NH2 modified anatase $TiO_2$ for effective photocatalytic degradation of azo dyes. Can J Chem Eng 95:1–9. https://doi.org/10.1002/cjce.22740

Lu M-C, Roam G-D, Chen J-N, Huang CP (1993) Factors affecting the photocatalytic degradation of dichlorvos over titanium dioxide supported on glass. J Photochem Photobiol A Chem 76:103–110

Makama AB, Salmiaton A, Saion EB et al (2016) Synthesis of CdS sensitized $TiO_2$ photocatalysts: methylene blue adsorption and enhanced photocatalytic activities. Int J Photoene. https://doi.org/10.1155/2016/2947510

Miller SM, Spaulding ML, Zimmerman JB (2011) Optimization of capacity and kinetics for a novel bio-based arsenic sorbent, $TiO_2$-impregnated chitosan bead. Water Res 45:5745–5754

Mohamed A, El-sayed R, Osman TA et al (2016a) Composite nano fibers for highly efficient photocatalytic degradation of organic dyes from contaminated water. Environ Res 145:18–25. https://doi.org/10.1016/j.envres.2015.09.024

Mohamed A, Osman TA, Toprak MS et al (2016b) Visible light photocatalytic reduction of Cr(VI) by surface modified CNT/titanium dioxide composites nanofibers. J Mol Catal A: Chem 424:45–53. https://doi.org/10.1016/j.molcata.2016.08.010

Mohamed A, Nasser WS, Osman TA et al (2017a) Removal of chromium (VI) from aqueous solutions using surface modified composite nanofibers. J Colloid Interface Sci. https://doi.org/10.1016/j.jcis.2017.06.066

Mohamed A, Osman TA, Toprak MS et al (2017b) Surface functionalized composite nano fibers for effi cient removal of arsenic from aqueous solutions. Chemosphere 180:108–116. https://doi.org/10.1016/j.chemosphere.2017.04.011

Mohamed A, Yousef S, Ali M et al (2017c) Photocatalytic degradation of organic dyes and enhanced mechanical properties of PAN/CNTs composite nanofibers. Sep Purif Technol 182:219–223. https://doi.org/10.1016/j.seppur.2017.03.051

Pan JH, Walcarius A, Pan JH et al (2010) Advanced materials for water treatment porous photocatalysts for advanced water purifications. J Mater Chem. https://doi.org/10.1039/b925523k

Peng S, Meng H, Ouyang Y, Chang J (2014) Nanoporous magnetic cellulose–chitosan composite microspheres: preparation, characterization, and application for Cu (II) adsorption. Ind Eng Chem Res 53:2106–2113

Salama A, Mohamed A, Aboamera NM et al (2017) Characterization and mechanical properties of cellulose acetate/carbon nanotube composite nanofibers. Adv Polym Technol. https://doi.org/10.1002/adv.21919

Salama A, Mohamed A, Aboamera NM et al (2018) Photocatalytic degradation of organic dyes using composite nanofibers under UV irradiation. Appl Nanosci 8:155–161. https://doi.org/10.1007/s13204-018-0660-9

Swaminathan S, Muthumanickkam A, Imayathamizhan NM (2014) An effective removal of methylene blue dye using polyacrylonitrile yarn waste/graphene oxide nanofibrous composite. J Environ Sci Technol. https://doi.org/10.1007/s13762-014-0711-z

Thunberg J (2015) Chemical modification of electrospun cellulose nanofibers. Chalmers University of Technology, Gothenburg

Uhl FM, Wilkie CA (2002) Polystyrene/graphite nanocomposites: effect on thermal stability. Polym Degrad Stab 76:111–122

Umar M, Aziz HA (2013) Photocatalytic degradation of organic pollutants in water

VanderHart DL, Hyatt JA, Atalla RH, Tirumalai VC (1996) Solid-state 13C NMR and Raman studies of cellulose triacetate: oligomers, polymorphism, and inferences about chain polarity. Macromolecules 29:730–739. https://doi.org/10.1021/ma9501860

Wang XH, Li J-G, Kamiyama H et al (2006) Wavelength-sensitive photocatalytic degradation of methyl orange in aqueous suspension over iron (III)-doped TiO$_2$ nanopowders under UV and visible light irradiation. J Phys Chem B 110:6804–6809

Wu F, Lu Y, Shao G et al (2012) Preparation of polyacrylonitrile/graphene oxide by in situ polymerization. Polym Int. https://doi.org/10.1002/pi.4221

Xiang C, Yang F, Li M et al (2013) Experimental and statistical analysis of surface charge, aggregation and adsorption behaviors of surface-functionalized titanium dioxide nanoparticles in aquatic system. J nanoparticle Res 15:1293

Yousef S, Mohamed A, Tatariants M (2018) Mass production of graphene nanosheets by multi-roll milling technique. Tribol Int 121:54–63

Yuan Y, Zhang G, Li Y et al (2013) Poly (amidoamine) modified graphene oxide as an efficient adsorbent for heavy metal ions. Polym Chem 4:2164–2167

Zaleska A (2008) Doped-TiO$_2$: a review. Recent patents Eng 2:157–164

Zhu Y, Murali S, Cai W et al (2010) Graphene and graphene oxide: synthesis, properties, and applications. Adv Mater 22:3906–3924